Remote Neuro-Cognitive Impairment Sensing based on P300 Spatio-Temporal Monitoring

Published Source:
D. De Venuto, V. F. Annese and G. Mezzina, "Remote Neuro-Cognitive Impairment Sensing Based on P300 Spatio-Temporal Monitoring," in IEEE Sensors Journal, vol. 16, no. 23, pp. 8348-8356, Dec.1, 2016, **doi: 10.1109/JSEN.2016.2606553.**

Remote Neuro-Cognitive Impairment Sensing Based on P300 Spatio-Temporal Monitoring

Daniela De Venuto, Valerio Francesco Annese and Giovanni Mezzina

***Abstract*— A novel mobile healthcare solution for remotely monitoring neuro-cognitive efficiency is here presented. The method is based on the spatio-temporal characterization of a specific event-related potential, called P300, induced in our brain by a target stimulus. P300 analysis is used as a biomarker: the amplitude and latency of the signal are quality indexes of the brain activity. Up to now, the P300 characterization has been performed in hospital through EEG analysis and it has not been experimented an algorithm that can work remotely and learn from the subject performance. The proposed m-health service allows remote EEG monitoring of P300 through a "plug and play" system based on the video game reaction of the subject under test. The signal processing is achieved by tuned residue iteration decomposition (t-RIDE). The methodology has been tested on the parietal-cortex area (Pz, Fz, and Cz) of 12 subjects involved in three different cognitive tasks with increasing difficulty. For the set of considered subjects, a P300 deviation has been detected: the amplitude ranges around 2.8−8 μV and latency around 300−410 ms. To demonstrate the improvement achieved by the proposed algorithm respect the state of the art, a comparison between t-RIDE, RIDE, independent component analysis (ICA) approaches, and grand average method is here reported. t-RIDE and ICA analyses report the same results (0.1% deviation) using the same data set (game with a detection of 40 targets). Nevertheless, t-RIDE is 1.6 times faster than ICA since converges in 79 iterations (i.e., t-RIDE: 1.95s against ICA: 3.1s). Furthermore, t-RIDE reaches 80% of accuracy after only 13 targets (task time can be reduced to 65s); differently from ICA, t-RIDE can be performed even on a single channel. The procedure shows fast diagnosis capability in cognitive deficit, including mild and heavy cognitive impairment.**

***Index Terms*— Mobile health-care, P300, t-RIDE, EEG, ERP.**

I. Introduction

NEUROLOGICAL disorder is a heavy cause of mortality. Among the neurological disorders Alzheimer disease (AD), Parkinson's disease (PD), Amyotrophic Lateral Sclerosis (ALS), Epilepsy, Mild Cognitive Impairment (MCI) and other dementias are estimated to constitute the 11.67% of total worldwide deaths (in 2005), and projections show an increment of 0.55% in the next 15 years, despite of drugs and specialized treatments [1]. Only in the US, 5.4 million people are affected by AD, with one new case appearing every 33 seconds [2]. The cost for providing care only for AD patients in the US was $200 billion in the 2012 and it is projected to grow to $1.1 trillion per year by 2050 [2].

Nowadays, the P300 analysis, which is a particular Event-Related brain Potentials (ERPs), is a widely used diagnostic tool for diagnosing and monitoring neuro-degenerative pathologies. It has been demonstrated that P300 latency and amplitude reflect the degree of cognitive decline [3]. The main problems related to the methods currently in use are: i) they are performed only in specialized centers scattered only in large urban centers; ii) the protocol to derive the P300 is time consuming (> 10 min) and when performed by electroencephalography (EEG) it requires the processing of at least 16 EEG channels (although recently some studies using 8 electrodes have been proposed [4], [5]). ERPs are usually analyzed using EEG and functional near-infrared spectroscopy (fNIRS) which are the leading non-invasive neuro-imaging solutions in terms of cost and portability [6]. While EEG offers a temporal resolution of about 0.05s and spatial resolution of ∼10 mm, fNIRS provides worst temporal resolution (∼1s) but higher spatial resolution (∼5mm) [7]. Many solutions have been already proposed in literature [8] for a correct and fast P300 extraction and detection starting from EEG raw data, in particular in Brain Computer Interface (BCI) applications [9]–[12]. Remarkable solutions involve the use of fNIRS for drowsiness detection while driving [6], EEG-based BCI experiment using Bayesian Spatio-Spectral Filter Optimization (BSSFO) [14]. Hybrid systems combining EEG and fNIRS have also been implemented to control a four directions mechanical arm in BCI applications [7]. However, since all these methods [6]–[13] are based on machine learning algorithms and on classification, they are not suitable as a diagnostic tool since their aim is only the detection of the P300 pattern but they are not oriented to P300 characterization in terms of amplitude, latency and brain area involved. For this reason, the most commonly used approach to measure and characterize the P300 in clinical environment are the Independent Component Analysis (ICA) [15], the Principal Component Analysis (PCA) [16] and the 'grand average'. Nevertheless, these approaches start their computations from some "a priori" assumptions that very often are not at all verified and valid for the P300. The application of mobile technologies for these analysis opens very interesting scenarios for new kind of approaches and investigations. The constant advances in personal electronic devices (PDAs) in terms of computational resources, mobile communication (3G, 4G, etc.) and cloud computing, together with the new wearable solutions, the fast decrease of the costs in consumer electronics, offer a number of

Manuscript received June 22, 2016; revised July 26, 2016; accepted August 22, 2016. Date of publication September 7, 2016; date of current version November 4, 2016. The associate editor coordinating the review of this paper and approving it for publication was Prof. Jun Ohta.

The authors are with the Department of Electrical and Information Engineering, Politecnico di Bari, 70125 Bari, Italy. (e-mail: daniela.devenuto@poliba.it; valeriofrancesco.annese@poliba.it; gmezzina23@gmail.com).

opportunities to create efficient mobile health-care (m-Health) solutions. M-Health is the new edge on healthcare innovation delivering health-care anytime and anywhere, surpassing geographical, temporal, and even organizational barriers with low and affordable costs [17]–[19], [21], [22], [29]. All the mentioned solutions can be successfully integrated into m-health systems favoring elderly care [20].

In this paper we present a novel EEG-based m-Health solution for neuro-cognitive impairment diagnosis. The tool is based on P300 spatio-temporal characterization, which is directly connected to the cognitive capability of the patient. The characterization is based on a tuned Residue Iteration DEcomposition (t-RIDE) approach optimized for P300 analysis which allows to extract spatial (topography, source of ERP, etc.) and temporal (latency, peak, etc.) parameters in order to detect neuro-cognitive impairment.

The solution represents the first implementation of a complete 'plug and play' automatic m-Health service, which allows remote data analysis. To the best of our knowledge, no EEG-based m-health system performing the remote cognitive impairment monitoring has been implemented in a single wearable tool. The main advantages of this m-health solution are: i) improved diagnosis results since the new algorithm for P300 characterization allows the tracking of subject clinical history; ii) the architecture knocks down geographical limits since the physician has access to data from everywhere and every time; iii) costs reduction for both the patient and the government, supporting domestic healthcare; iv) improvement in the life quality of the patients, which can be tested and treated at home (beneficial for people affected by PD, AD, ALS). Summarizing, the novel test procedure takes just few minutes (i.e.: the response is almost in real time), and the analysis equipment is non-invasive and just needs few EEG channels. The paper structure is outlined in the following: Section II provides basic knowledge on the P300 features and briefly outlines the state of the art for its automatic detection; Section III describes the novel m-Health architecture and details the t-RIDE algorithm. Section IV presents the experimental results coming from in vivo measurements on 12 subjects (age 26.5±3.5), focusing on both the algorithm performance and the P300 spatio-temporal characterization. Section V concludes with final observations.

II. Evoked Related Potentials

A. Evoked Related Potential: The P300

The P300 is a positive deflection in the human brain event-related potentials (ERPs) evoked when a subject is actively and cognitively engaged in the discrimination of one target stimulus by not-target ones (Fig 1) [23], [24]. In literature [24], 'stimulus' is a single external event (audio, visual, tactile, etc.) delivered to the subject under test. The target stimulus is the event to be recognized among different ones (not-target). A game/task is an assemble of stimuli (target and not-target ones). The nature of the external event to the P300 occurrence is irrelevant (we used visual stimuli), but, in a single task, the probability of target occurrence has to be lower than the not-target one. This well-consolidated procedure is generally known as the "oddball" paradigm [23], [24]. The P300 characterization is mainly based on: the latency, the amplitude of the detected pulse, the location and the source. The P300 latency is heavily affected by trial-to-trial variability (P300 jitter) within a given experimental condition and, according to [25], ranges from 290ms to 447.5ms depending on the cognitive difficulty of the discrimination. The P300 amplitude is considered as the peak-to-peak amplitude between the previous deflection (N200) and the P300 maximum value (see Fig. 1). According to [25], P300 amplitudes can reach even 37.7μV depending on the age and on the rarity of the target stimulus. The intracerebral origin of the P300 wave is not known and its role in cognition not clearly understood. Generally, the P300 is more clearly detectable in the central parietal cortex [23]. The brain mapping of P300 is computed by a topography.

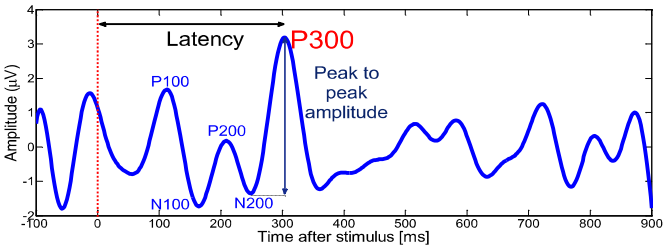

Fig. 1. Evidence of P300 experimentally obtained from an healty subject on PZ.

TABLE I
Clinical P300 Reference for Diagnonis

	Amplitude [μV]	Latency [ms]	FoM [μV/ms]
Healthy	>5.3	< 349	≥ 0.01
MCI[1]	1.4 < A < 3.1	>389	0.003≤FoM≤0.008
HCI[2]	< 1.4	>400	FoM≤0.003

[1] Mild Cognitive Impairment; [2] Heavy Cognitive Impairment

B. P300 as Biomarker for Cognitve Impairment Diagnosis

P300 latency and amplitude reflect the degree of cognitive decline in dementing illness [3]. A single P300 pulse is anticipated by further ERPs (i.e. P100, N100, P200 and N200 – see Fig. 1) which classify the cognitive process. The P300 characterization as biomarker for cognitive impairment is based on the simultaneous evaluation of amplitude and latency. For this aim, the proposed m-Health tool identifies a new figure of merit (FoM), defined as:

$$FoM = \frac{Peak\text{–}to\text{–}Peak(P300\text{–}N200)}{Latency}_{[\frac{\mu V}{ms}]} \quad (1)$$

where the relative peak distance between P300 and N200 potentials are considered. According to [26], it is possible to extract threshold values for amplitude and latency for 26 healthy subjects (aged 64.9 ± 10.9 years), the P300 amplitude is > 5.3μV, the latency < 349ms [26]. From these clinical values, we estimated that for healthy subject the FoM is > 0.01 μV/ms. FoM ranging between 0.008μV/ms<FoM<0.01 μV/ms, defines potentially healthy subjects. Table I reports threshold values according to [26].

C. Brief Review of the Automatic P300 Detection Methods

Plenty of methods have been presented in literature for P300 detection in single-trial and averaged-trials environments [4]–[13], [27], [28]. Nevertheless, the use of conventional ERP averaging (grand average) is inappropriate since the intrinsic variability of the ERP leads to distortions of latencies, reduction in maximum amplitude (peak) and a broadening of the component.

Woody in [27] suggested a method for single-trial ERPs, based on an iterative strategy. At first, the latencies are estimated from the cross-correlation between the grand average (first template) and each trial. Then, all single-trials are aligned to the estimated latency and averaged again, leading to a second template. Finally, those steps are re-iterated until the templates convergence. The main limitation of this approach is the hypothesis that the ERP is monolithic (only latency jitter without shape distortion) which is not verified in the reality. Other latency detection methods (i.e. peak-detection) face the same problem. Different approaches such as independent component analysis (ICA) [15] and principal component analysis (PCA) [16] need a starting assumptions on the amplitude and latency value and need to monitor a high number of EEG electrodes. ICA assumes that there are independent sources generating signals, which are projected to the scalp [15]. Nevertheless, the source of P300 is not known a priori resulting in the impossibility to apply this method for this particular ERP. PCA, instead, separates the signal into orthogonal components but the limitation of this methods leads into the assumption of amplitude variation within trials excluding latency jitter [16]. A further class of methods are based on deconvolution. Those approaches attempt to separate stimulus-locked and response-locked ERP component assuming a linear model of ERP interaction. Specifically, the ERP is de-convoluted into – at least – two ERP components, one stimulus-locked s(t) and one response-locked r(t). The main limitation of this model is the undesired amplification of slow noise components (≈1Hz). Since the ERP alignment is performed by using the physical response of the subject (go-tasks) to the target as the time-base, de-convolutive methods fail to find latency jittered components in tasks with no external response (no-go tasks), which is our situation. The method adopted in this work is a tuned version of the residue iteration decomposition (RIDE) which is a hybrid approach based on linear superposition and iterative residual calculation [29]. The RIDE allows to detect spatio-temporal ERP characteristics with no limitations in terms of number of electrodes and number of target stimuli.RIDE considers a linear superposition model of single-trial ERPs. Except for the noise ε, the single-trial EEG is decomposed into two components: stimulus-locked (S) and cognitive-locked (C) components. In go-task, i.e. task in which the subject is asked to perform a motor action, a third component response locked (R) has to be considered (but this is not our case). A single-trial EEG, including EEG background activity and noise, can be expressed as:

$$EEG_i(t) = S(t) + C(t+\tau_i) + \varepsilon(t) \tag{2}$$

Where τ_i is the latency of component C in the i-th trial and is characterized by a distribution $\rho(t)$ assumed to be Gaussian (but this is not a limitative hypothesis). A conventional average over N trials would result in:

$$\begin{aligned}\langle ERP\rangle &= S(t) + \frac{1}{N}\sum_{i}^{N} C(t+\tau_i) + \frac{\varepsilon(t)}{\sqrt{N}} = S(t) + \int C(t+\tau)\,\rho(\tau)\,d\tau \\ &+ \frac{\varepsilon(t)}{\sqrt{N}} = S(t) + C * \rho + \frac{\varepsilon(t)}{\sqrt{N}}\end{aligned} \tag{3}$$

Equation 3 shows that, although noise is reduced, the average creates a broadening of the C component which is convolved with its distribution. Neglecting ε, it is possible to consider the residues in single-trial:

$$Res_i(t) = EEG_i - \langle ERP\rangle = C(t+\tau_i) - C * \rho \tag{4}$$

If the residues are aligned to their τ_i through cross-correlation jitter-latency estimation and averaged again, the distortion are reduced and a first estimation of C is computed as:

$$C_1(t) = < Res > = C(t) - (C * \rho) * \rho \tag{5}$$

By replacing C_1 in (3), it is possible to obtain a first estimation of S_1. The procedure is then iterated using a first ERP estimation [$ERP_1 = S_1(t) + C_1(t+\tau_1)$] leading at the end to a more precise S and C estimation. After the n-th iteration, the components C_n and S_n are given by:

$$C_n(t) = C - C * \rho_0 * \rho_1 \ldots\ldots * \rho_n \to C \tag{6}$$

$$S_n(t) = S - S * \rho_0 * \rho_1 \ldots\ldots * \rho_n \to S \tag{7}$$

After n iterations, C_n and S_n converge to C and S since the iterative convolution by ρ approaches to zero. Differently from similar iterative methods (i.e. Takeda et al. [28]), the RIDE method does not introduce systematic artifacts and its convergence is fast (≈ 10 iterations). The RIDE algorithm has been tested for different trends of ρ and it has been verified to be robust and accurate [29]. Due to RIDE advantages which comprise low number of target stimuli, no-go task applicability, few electrodes needed, good accuracy, information regarding single-trial, etc., the RIDE method was selected as core for our diagnostically tool but has been fine tuned for P300 detection (t-RIDE).

III. System Architecture

The system is made up by two sides: the patient and the medical ones, which communicate each other by cloud technology using TCP/IP connection. Fig. 2 summarizes the overall architecture. In the implemented solution, the patient wearing a wireless EEG headset, can perform autonomously at home three different oddball tasks of increasing cognitive difficulty on a PC, tablet or smartphone. The tests are completely driven by the software, which is totally 'plug and play' and no user intervention is needed. The oddball protocol (described in detail in the next sections) and the t-RIDE parameters are based on a configuration file (.txt) which is cloud-shared with the medical center in order to be eventually

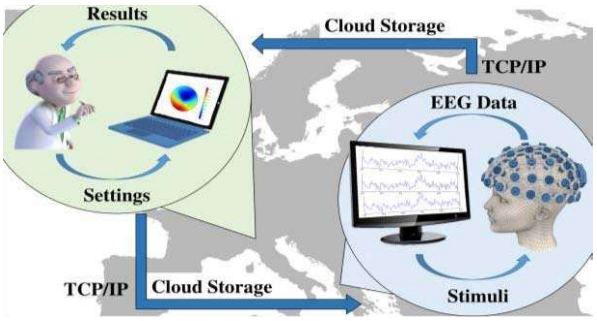

Fig. 2. Overall architecture of the m-Health service proposed.

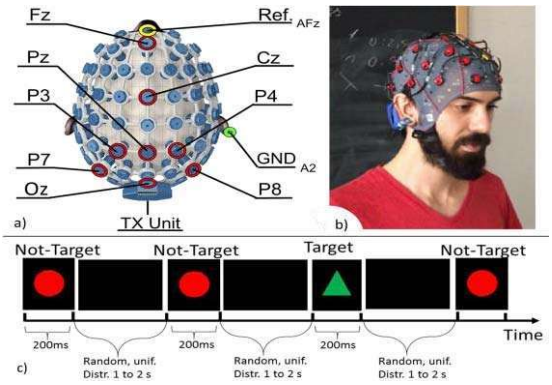

Fig. 3. a) Channels of interest (in red) according to the international system 10-20. In yellow the nasion reference and in green the ear-lobe ground. b) Demontrative picture of the EEG wireless headset. c) Time diagram of task A.

modified by the physician. EEG data are immediately in-loco processed by t-RIDE and the consequent medical report (in pdf format) is created and, in real time, cloud-shared with the physician. The report contains the spatio-temporal P300 characterization. The physician, then, basing on the data and on the clinical history of the patient (the previous output files are never deleted) performs a personal diagnosis. In case of cognitive impairment monitoring, the physician can, for instance, remotely verify the effectiveness of a drug treatment. In case of periodical analysis for predisposed subject, the physician can detect the early presence of neuro-impairment. It should be pointed out that the m-Health system only performs accurate measurements and data processing but the final diagnosis is left to the human component of the m-Health service (medical center, physician, etc.).

A. The Hardware

The patient side equipment is: i) the EEG wireless headset (sensors and gateway), ii) the PC or tablet, etc. with TCP/IP connection, iii) the test game (stimuli delivering) defined with the medical center and iv) a user-friendly software, which collects data, analyzes (by t-RIDE) and uploads them on the cloud. The patient side performs data collection and P300 detection: EEG data collected by the wireless EEG headset are sent to the gateway (i.e. PC) which delivers the video game/test and performs EEG processing. Once processed, the results are uploaded on the cloud and made available for the medical center. In our experiments, the EEG headset is a 32-channels wireless recording system exploiting active electrodes (conditioning integrated circuit are embedded in the electrode performing amplification, filtering and digitalization). The EEG headset is the g.Nautilus commercial device by g.Tec. According to the international 10-20 system for the EEG, eight channels are considered (Fz, Cz, Pz, Oz, P7, P3, P4, P8 – in red in Fig. 3.a) referenced to AFz (in yellow) while the right ear lobe (A2) is used as ground (in green). EEG signals are recorded during the test and are synchronized with the delivered stimuli by the gateway, which drives the test. The gateway is a PC with proper wireless communication interfaces for the BLE link and an efficient wide-area communication interface (i.e. TCP/IP). We used a PC (Intel i5, RAM 8 GB, 64 bit) [23], [30], [31]. EEG data collection, the game/stimuli generation and subsequent data processing are performed by Simulink. Once the P300 processing is completed, output files are delivered both to the patient (immediate response) and to the physician, which constitutes the decision-maker and, by visual inspection, can perform a remote diagnosis basing on t-RIDE measures. The medical side of the m-health consists of: i) the personal electronic device (PC, tablet, etc.), ii) the configuration file for the signal processing to be loaded on the cloud and iii) the clinical database stores all datasets describing the medical history of the patient. The physician has a two possibility of interaction with the system: on one hand, he can modify the cloud-shared parameter file (.txt) which is loaded by the gateway before each test and contains directives both for tasks both for signal processing (i.e. window of interest, channels, etc.); on the other hand, the physician can consult the results of the test. The results are the spatial (topography i.e. brain mapping) and temporal (latency, peak, etc.) characterization of the occurred P300. Those are cloud-stored and the physician has always access to clinical records of the patient in order to evaluate his medical history. In this way, the evaluation of the evolution of the neuro-cognitive impairment can be evaluated. Data security will be guaranteed by proper-compounded authentication systems (i.e. fingerprint or double password).

B. The Cognitive Tasks (Oddball Test)

The remotely performed cognitive tasks are based on the oddball paradigm [24] and are delivered by the gateway through visual stimuli (videogame). The patient performs three different no-go cognitive tasks (task A, B and C) of increasing difficulty, where he has to recognize the rare target stimuli among the not-target ones. Before each task, for a 20s slot no stimuli are presented in order to allow the run out of the filter effect.

Task A. On a black screen (15”), a red circle and a green triangle are repeatedly and randomly flashed. The subject is asked to count in mind the occurrence of the less frequent target stimulus, which is the green triangle. The flashing stimuli are randomly presented with non-uniform probability: the target stimulus probability is 20%. The inter-stimuli time is randomized and has a uniform distribution ranging from

1 to 2 seconds. Each visual stimulus persist on the screen for 200ms. The subject distance to the screen is approximately 1.5m.

The time length of task A is 127s (approx. 25 target stimuli presented). Since task A involves both chromatic and geometrical mental classification, the P300 is expected to be more evident. In Fig. 3.c a time-diagram of task A is presented.

Task B. The protocol of task B is the same as task A but the flashed visual stimuli are different. There is no more chromatic classification: a red triangle (target stimulus with 20% probability of occurrence) and a red circle (not-target stimulus) are randomly delivered to the subject. The cognitive difficulty for task B is increased since the human brain classification is only based on the geometrical shape.

Task C. Task C preserve all the configuration of task B but the classification based on the geometrical shape is made more difficult by the presence of stimuli with very similar shapes (not-target: red circle; target: red ellipse).

Task A has been developed according to medical standard protocols and aims to verify that t-RIDE results match the literature reference [24], [26]. Task B and C have been developed to verify and quantify the degradation of P300 [3].

C. The Software: Spatio-Temporal P300 Characterization

The main software driving the m-Health system, managing data collection, delivering the test, processing the data and providing the cloud-communication is a Simulink-based application.

1) Data Collection: A dedicated Simulink block for data collection managing the API of the headset has been developed. Data are sent to the gateway trough Bluetooth low energy (BLE) protocol. The above mentioned eight EEG electrodes (Fz, Cz, Pz, Oz, P7, P3, P4, P8) are recorded at 500Hz, with 24-bit resolution, input range ±187.5mV and filtered using a bandpass (Butterworth, 8th order 0.5-100Hz) and a notch (Butterworth, 4th order 48-52Hz) filters. Those filters are embedded into the signal conditioning circuit of the EEG electrodes. The recording scheme is monopolar and the frame length is 8 [23], [30]–[33].

2) Cognitive Test: As soon as the test is lunched (the software is 'plug and play' i.e. the subject just have to wear the EEG headset, select the task and press 'play'), after a 20 s wait time, the visual test/game is delivered on the monitor.

The stimuli are controlled by a numeric signal, which controls a multiplexer and provides to the video device the selected image. EEG data and the numeric signal driving the test/game are stored. At the end of the task, t-RIDE starts automatically.

3) Signal Processing: The automatic P300 spatio-temporal characterization is based on a tuned version of the RIDE approach (t-RIDE) optimized for P300 analysis. The signal processing, schematically outlined in Fig. 4, is a three stage approach which involves pre-processing, t-RIDE application for P300 characterization, output preparation and sending. The signal processing is performed for each monitored channels and derivative channels obtained by averaging different electrodes. In the following, a single-channel processing chain is outlined.

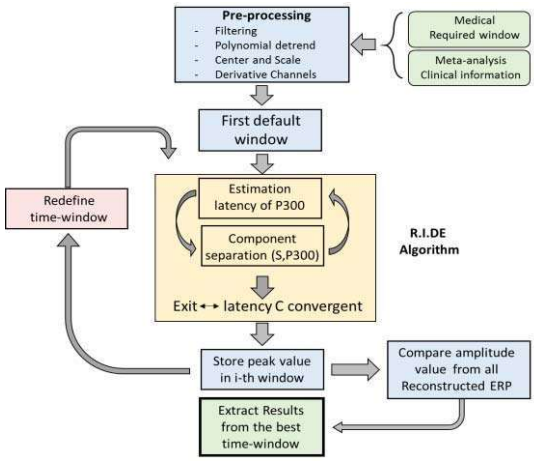

Fig. 4. Schematic flow-chart of the signal processing. The signal processing is applied to each channel monitored and derived signals.

4) Pre-Processing: The signal collected by the gateway is further low-pass filtered (Butterworth, 6^{th} order, $f_{stop} = 15$Hz) and aligned to the stimulus signal. This is a further numeric filter and (different from the previous mentioned ones). Subsequently, EEG signal is decomposed into epochs of 1s: each epoch starts 100ms before the rising edge of the stimulus (target and not-target) and ends 900ms after it. Epochs are fitted into a 6^{th} order polynomial curve. The selected polynomial order is the highest one able to eliminate of the slow bias drift without modify the ERP patterns. The resulting curve fitting is subtracted to the EEG signal, which is then centered (offset cancellation) and normalized. Thus, the pre-processing is completed and signals are ready to be processed.

5) t-RIDE: The t-RIDE algorithm is made up by two phases: i) window optimization and ii) results extraction. RIDE algorithm is a generic approach for ERP extraction but it needs to be tuned for P300 calculation. In order to reduce the computational effort and since it is not known 'a priori' the source of P300, at first only one signal derived from the average of P_z and C_z is considered for the window optimization. A first default rectangular window is set to 250 ms – 400ms after the target stimulus. The first window sizing can be customized by the physician. A starting estimation of the latency C is performed using the Woody's Method and a first characterization of the P300 is performed [27]. Based on template matching, the cross-correlation between the template of P300 and a single trial EEG is performed and residuals are calculated separating the S and C components. The procedure is iterated until the latency C in single trials stops changing monotonically. When the C latency convergence is reached, the results are stored and the procedure is iterated again with a different windowed EEG signal. The start of the window is iteratively 4ms right shifted while the end of the window performs 8ms right shift. Seven different windows are considered in order to cover the full time range in which the P300 can occur [25]: the last computation is performed on the rectangular window of 278 – 456ms after target stimulus. At each iteration, the evaluated P300 maximum amplitude

related to the particular used window is stored. At the end of the window definition cycle, the window that has led to the highest P300 peak is considered the optimized window. After the window optimization phase, the procedure for results extraction is performed on all the pre-processed channels. The results extraction phase involves the application of the RIDE method on the optimized window previously computed. For each channel, the P300 is totally reconstructed in the window hooking the S component to rising edge of the target stimulus, while the C component is appended to S using the estimated value of its latency.

6) Outcomes: For each channel, information about latency and peak are presented. The presented approach needs to estimate the latency of the C component (which coincides with the P300) for each single-trial so information about latency and peak variation trial-by-trial can be estimated. A statistical analysis of the data informs the physician of the medium latency and peak. The P300 characterizing output files are automatically stored on the cloud and consists of:

i) Diagrams showing the time-domain waveforms of target stimuli compared to no-target for each channel and task;

ii) Maps showing information on the P300 generation and propagation for each task (topography);

iii) An automatically generated table that expresses presence/absence of P300, peak values and latency values for each channel and task.

The software contextually presents the same data in loco to the care-givers and to the patient, but does not express any formal diagnosis, which will be performed by the specialized physician.

IV. Results

The dataset is based on recordings for ethical reason, on 12 healthy subjects (aged between 23 and 30) acquired with a wireless equipment and supported by highly specialized medical staff. The group was selected in consideration of a certain degree of homogeneity in terms of age and level of education. Recordings were performed in a controlled environment. Subject were asked to perform task A, B and C minimizing eye movements, blinking, head and body movements, jaw contraction, etc. in order to reduce artifacts.

A. P300 Spatio-Temporal Characterization

In the upper part of table II, the results on the complete dataset for each task are presented. For task A, the P300 amplitude range was 3 - 8 μV with a mean value of 4.7μV $\pm$ 0.61μV; the P300 latency in task A was included in the range 300 – 403ms, with a mean value of 349.25ms $\pm$ 35.52ms. For task B, the amplitude mean value was 4.4μV $\pm$ 1.28μV ranging in 3 - 6.2μV; the latency range was 340-410ms and its mean value was 363.3ms $\pm$ 14.91ms. For task C, the mean amplitude was 3.7μV $\pm$ 0.98μV in the 2.8-4.9μV range; the mean latency was 378.46 ms $\pm$ 14.91ms. The average latency increases from task A to C was +7.7%; the average P300 peak decreases from task A to C was -21.28%. P300 amplitude and latency for each subject performing all the tasks are reported in figure 5, which shows

TABLE II

Results of t-RIDE Compared to Related Works

Dataset	Method	Subjects	P300 Peak	P300 Latency
Task A	t-RIDE, 25 Average targets, 8 channels	12, healthy (age 26.5 ±3.5)	Range : 3-8 µV Mean : 4.7 µV σ : 0.61	Range: 300-403 ms Mean : 349.25ms σ : 35.52
Task B	t-RIDE 25 Average targets, 8 channels	12, healthy (age 26.5 ±3.5)	Range : 3-6.2µV Mean : 4.4 µV σ : 1.28	Range : 340-410ms Mean : 363.3ms σ : 14.97
Task C	t-RIDE 25 Average targets, 8 channels	12, healthy (age 26.5 ±3.5)	Range : 2.8-4.9 µV Mean : 3.7 µV σ : 0.98	Range : 360-410ms Mean :378.46 ms σ : 14.91
Related work [25]	Mix, > 160 targets	75, healthy (age: 27,17± 19.16)	Range : 2.6-37.7 µV Mean: 10.4 µV σ : n.d.	Range : 290-447 ms Mean : 316.5 ms σ : n.d.
Task A	RIDE, 25 Average targets, 8 channels	12, healthy (age 26.5 ±3.5)	Range : 2.2 - 7 µV Mean : 4.1 µV σ : 1.43	Range: 302-387 ms Mean : 351.4ms σ : 36.13

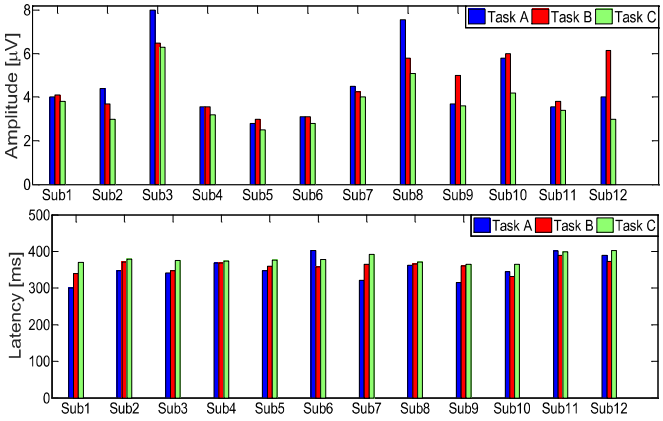

Fig. 5. P300 amplitude (top) and latency (bottom) evaluated using t-RIDE on 12 subjects performing three tasks of increasing difficulty. Increasing the cognitive difficulty of the task, latency increases while amplitude decreases.

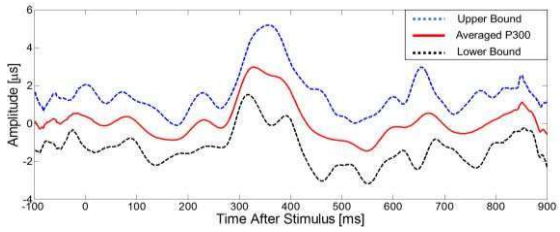

Fig. 6. Averaged P300 (task A on Pz) of all the 12 subjects (in blue), upper (blue) and lower (black) bounds depicting one standard deviation.

also the P300 degradation: increasing the task complexity P300 amplitudes decrease while latency times increase, as already presented in table II. The latency increment from task A to C was +7.7%; the average P300 peak decrement from task A to C was −21.28%. In the 100% of the recordings, P300 had a higher amplitude in presence of the target than for the not-target one (average $\Delta V = 2.95\ \mu V \pm 1\ \mu V$ on Pz). Figure 6 shows the subject-to-subject P300 variability by averaging 12 P300 pulses from the subjects under test on Pz during task A (in red). The upper and lower boundary layers depicting a standard deviation are shown, respectively, in blue and black. This analysis confirms that, for all subjects

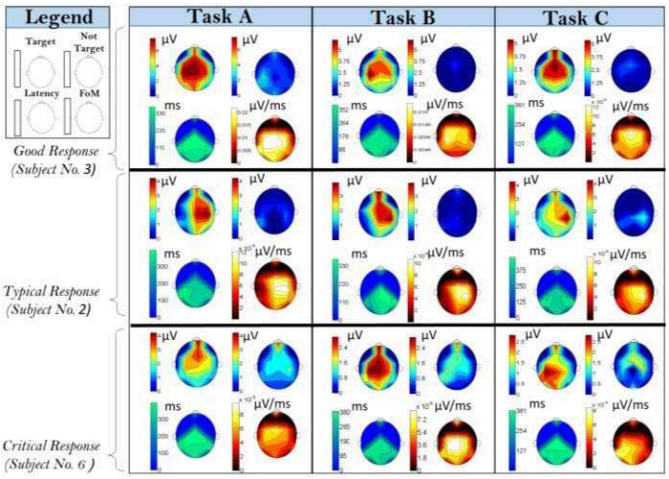

Fig. 7. t-RIDE results for each task for 3 different subject performing good, typical and critical response. Clockwise, starting from the top left corner of each cell we present the target, not-target, FoM and latency topographies. P300 was P300 is more evident in the central-parietal electrodes.

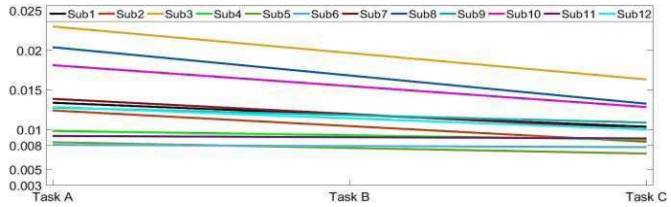

Fig. 8. FoM behavior with increased difficulty of the cognitive task.

the P300 peak occurs around 300ms. Figure 7 shows the topographies of the amplitudes (for both target and not-target stimuli), latencies and FoM for 3 different subject performing task A, B and C. The results shown in the figure have been selected in order to highlight three different P300 responses: good response (high FoM, sub. no. 3), typical response (average FoM, sub no. 2) and critical response (low FoM, sub no. 6). The P300 highest voltage levels (in the target amplitude topography) are concentrated in the center-parietal region (Cz, Pz, P3, P4). From the latency topography it is shown that the P300 is detected from the lateral mid-line electrodes (200-250ms on P3 and P4) and the central electrodes (Fz, Cz, Pz) 300-400 ms after stimulus. The FoM analysis allows characterizing the subject from both amplitude and latency at the same time. The highest values of FoM are recorded in the parietal cortex (Pz, P3, P4, P7 and P8). As shown in Fig. 8, the 100% of the subject showed FoM reduction with the increased difficulty of the task. In particular FoM decreases (in average) from 0.0135 μ V/ms $\pm$ 0.005 (task A) to 0.012 μV/ms $\pm$ 0.004 (task B) until 0.011 $\pm$ 0.003 (task C).

B. t-RIDE Results and Method Validation Respect the State of the Art Methods

In Table II, reference analysis are reported. The authors in [25] describe that on 75 healthy subjects (age 27.17 $\pm$ 19.16, covering the lifespan) the P300 amplitude varies between 2.6μV and 37.7μV with a mean value of 10.4μV, while the P300 latency ranges from 290ms to 447ms

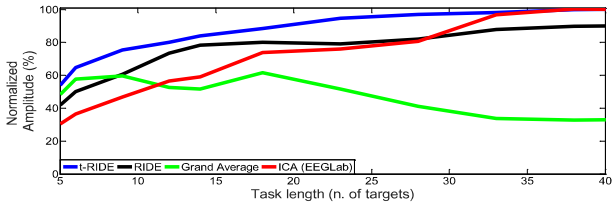

Fig. 9. P300 amplitude calculated using: t-RIDE (in blue) RIDE (in black), GA (in green), ICA (in red). The analysis is referred to identical dataset and on a single channel Pz.

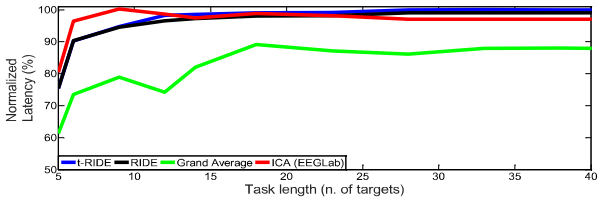

Fig. 10. P300 latency calculated using: t-RIDE(in blue), RIDE (in black), GA (in green), ICA (in red). The analysis is referred to identical data and on a single channel Pz.

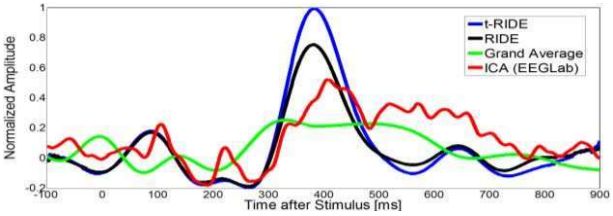

Fig. 11. P300 extraction from subject 1 during task A using t-RIDE (in blue), RIDE (in black), Grand average (in geen), ICA (in red). To simplify the plot only Pz is shown. 25 targets were considered.

with a mean value of 316.5ms. Note that [25] is a review of 75 different papers, which implement several P300 extraction methodologies. For each task and subject, the 100% of t-RIDE results were consistent with the reference, confirming the validity of the approach. By comparison between RIDE and t-RIDE results it is possible to observe (table II) that t-RIDE calculated P300 peak is, in average, +0.6 μV (+12.76%) higher than the one calculated by RIDE. Comparing the standard deviations, t-RIDE performs +57.34% higher accuracy: $\sigma_{\text{t-RIDE}} = 0.61$, $\sigma_{\text{RIDE}} = 1.43$. Concerning latency estimation, the two methods reports very similar results. In figures 9, 10 and 11, a comparison between t-RIDE, RIDE, ICA and Grand Average (GA) is presented. ICA and GA are the most commonly used methods nowadays in specialized medical centers for P300 extraction. The above mentioned methods were applied on identical data stream (subject 1, Task A; 8 channels). In figure 9 and 10 the amplitude and latency were normalized according to the eq. (8):

$$\varepsilon_{\text{n},\%} = \frac{|x_{N-}\Delta x_n|}{x_N} \cdot 100;\ \Delta x_n = \left|x_{N-}\hat{x}_n\right| \tag{8}$$

Where x_N is the P300 amplitude/latency evaluated with t-RIDE using a task with N = 40 target stimuli, $\hat{x}_n$ is estimated over n target stimuli, with n < N. x_N is the convergence of the method (steady state value), and can be used as a reference value to

evaluate the accuracy of the calculation, when n < N targets are used. Notice that, under this assumption, ε_n is also the accuracy of the measurement. Figure 9 shows the convergence of P300 amplitude achieved by the considered methods with increasing the number of target stimuli within the same task. The amplitude has been normalized to the "steady state" value achieved by t-RIDE using 40 targets, according to eq. (8). Figure 9 shows that:

i) **t-RIDE and ICA converge to the same results for the amplitude** with an error of 0.1%;

ii) **t-RIDE is, in average, +12.3% more accurate than RIDE** although they exhibit the same converge trend;

iii) The GA converge value was 67% lower than t-RIDE;

iv) **For amplitude, t-RIDE is more accurate than the competitors.** t-RIDE showed the highest accuracy using 25 targets: t-RIDE = 96.05%; RIDE = 78%; ICA = 75.9%; GA = 51.6%;

v) **t-RIDE needs less targets to reach 90% amplitude accuracy if compared to the existing methods.** The number of target stimuli to reach 90% accuracy are: t-RIDE = 18; RIDE = 38; ICA = 30; GA = n.d. (GA never reaches 90% accuracy). Notice that for task A, the probability of target occurrence was 20%. Considering 1s inter-stimulus time, rough conversion between number of targets and time duration of the task can be done: 1 target $\approx$ 5s. That means, in order to extract the P300 amplitude with a 90% accuracy, the time duration of the task has to be: t-RIDE = 90s; ICA = 150s; RIDE = 190s. Clearly, **an oddball task design to be used with t-RIDE has a shorter duration.** This heavily reduces the habit phenomenon (which degrades the P300), improving the comfort for the patient.

Figure 10 shows the convergence of P300 latency achieved by the considered methods with increasing the number of target stimuli within the same task. The latency has been normalized according to eq. (8). Figure 10 shows that:

i) **t-RIDE, ICA and RIDE converge to the same results for the latency;**

ii) For latency, **t-RIDE is, in average, +1% more accurate than RIDE +3% more accurate than ICA** and although they exhibit the same converge trend;

iii) The GA converge value was 12% lower than the t-RIDE;

iv) **For latency, t-RIDE needs the same number of targets to reach 90% accuracy if compared to ICA and RIDE:** t-RIDE = 6; RIDE = 6; ICA = 6. The number of targets to reach 90% accuracy for latency calculation with GA is 18. t-RIDE analyzes the EEG channels individually: the minimum EEG channels for t-RIDE is 1. Contrariwise, ICA requires a great number of electrodes: more than 32 channels are suggested [15]. The minimum EEG channels for ICA is 6. t-RIDE adoption allows to wear a more comfortably headset since there is no minimum required number of channels and 90% accuracy is reachable even with a single channel.

Computationally speaking, **t-RIDE is 1.6 times faster than ICA.** t-RIDE convergence is reached in 79 iteration (i.e. 1.95s) on a single EEG channel. With the same dataset, ICA convergence to the same result is reached in 216 iteration (i.e. 3.1s) giving 80% accuracy with 28 targets. Fig. 11 presents the time-domain P300 waveform on Pz calculated using the above mentioned methods using subject 1, task A, 25 targets.

C. Discussion on Cognitive Impairment Detection

t-RIDE results of task A are compared to clinical reference values in table I (because the control groups defined in [26] were measured using a paradigm very similar to task A). Task B and C have been developed to demonstrate and quantify the P300 degradation increasing the task difficulty. However, the diagnosis and decision is always left to the human component of the m-Health service i.e. the physician, especially for critical situations i.e. subject 6 which performed for task A, a FoM = 0.008 μV/ms (on the edge of the clinical groups). According to fig. 10 and 11, the FoM calculation by ICA or RIDE reports the same results but with higher number of target to reach 90% of accuracy (t-RIDE: 18; ICA: 30; RIDE: 38) resulting in a longer game/test (t-RIDE: 90s; ICA: 150s; RIDE: 190s). Furthermore, t-RIDE can be performed even on a single channel.

V. Conclusion

A novel m-health solution for neuro-cognitive impairment monitoring based on P300 spatio-temporal characterization achieved by tuned Residue Iteration Decomposition (t-RIDE) has been presented. To the best of our knowledge, this is the first solution performing this kind analysis and represents a breakthrough in the field of cognitive diagnosis and monitoring. The architecture is supported by a new method for P300 analysis which overcomes the limitations of the previous approaches (ICA; PCA; grand average; etc.). The developed t-RIDE method has been here validated on a dataset of 12 subjects performing three different cognitive tasks of increasing difficulty. The algorithm is very efficient: the convergence is reached in 79 iterations in 1.5s and its robustness has been tested also decreasing the number of trials taken into account. The m-health service proposed, allows remote monitoring of neuro-cognitive impairment through a 'plug and play' application, while physician customization and data collection are allowed by cloud bridging.

Acknowledgments

The authors would like to thank the Medical Center "Giovanni XXIII" and the neurological research team headed by Prof. De Tommaso and Eng. Sabino Loconte for his collaboration during data collection.

References

[1] The World Health Organization (WHO), "Neurological disorders. Public health challenges," World Health Org., Geneva, Switzerland, Tech. Rep., 2006. [Online]. Available: https://books.google.it/books?hl=it&lr=&id=Z8uwPwlPUw4C&oi=fnd&pg=PR1&dq=neurological+disorders+public+health+challenges.+geneva+world+health+organization+2006&ots=gfsDz2YsSj&sig=Q1Pf8Oz_0Pbr2eM8x9kl1RumhdQ#v=onepage&q=neurological%20disorders%20public%20health%20challenges.%20geneva%20world%20health%20organization%202006&f=false

[2] M. Prince *et al.*, "World Alzheimer report 2015: The global impact of dementia," Alzheimer's Disease Int., London, U.K., Tech. Rep., 2015. [Online]. Available: https://www.alz.co.uk/research/WorldAlzheimerReport2015.pdf

[3] J. Polich, C. L. Ehlers, S. Otis, A. J. Mandell, and F. E. Bloom, "P300 latency reflects the degree of cognitive decline in dementing illness," *EEG Clin. Neurophysiol.*, vol. 63, no. 2, pp. 138–144 1986.

[4] A. Turnip and K.-S. Hong, "Classifying mental activities from EEG-P300 signals using adaptive neural network," *Int. J. Innov. Comput. Inf. Control*, vol. 8, pp. 6429–6443, Sep. 2012.

[5] D. De Venuto, M. J. Ohletz, and B. Riccò, "Digital window comparator DfT scheme for mixed-signal ICs," *J. Electron. Test., Theory Appl.*, vol. 18, no. 2, pp. 121–128, 2002, doi: 10.1023/A:1014937424827.

[6] M. J. Khan and K. S. Hong, "Passive BCI based on drowsiness detection: An fNIRS study," *Biomed. Opt. Exp.*, vol. 6, no. 10, pp. 4063–4078, 2015.

[7] M. J. Khan, M. J. Hong, and K. S. Hong, "Decoding of four movement directions using hybrid NIRS-EEG brain-computer interface," *Frontiers Human Neurosci.*, vol. 8, p. 244, Apr. 2014.

[8] F. Lotte, "A review of classification algorithms for EEG-based brain-computer interfaces," *J. Neural Eng.*, vol. 4, no. 2, pp. R1–R13, 2007.

[9] V. D. De, M. J. Ohletz, and B. Riccò, "Testing of analogue circuits via (standard) digital gates," in *Proc. Int. Symp. Quality Electron. Design (ISQED)*, Jan. 2002, p. 112, doi: 10.1109/ISQED.2002.996709.

[10] N. Naseer and K.-S. Hong, "fNIRS-based brain-computer interfaces: A review," *Frontiers Human Neurosci.*, vol. 9, p. 3, Jan. 2015.

[11] L. M. McCane *et al.*, "Brain-computer interface (BCI) evaluation in people with amyotrophic lateral sclerosis," *Amyotrophic Lateral Sclerosis Frontotemporal Degenerat.*, vol. 15, pp. 207–215, Jun. 2014.

[12] K.-S. Hong and H.-D. Nguyen, "State-space models of impulse hemodynamic responses over motor, somatosensory, and visual cortices," *Biomed. Opt. Exp.*, vol. 5, no. 6, pp. 1778–1798, Jun. 2014.

[13] H.-I. Suk, "Predicting BCI subject performance using probabilistic spatio-temporal filters," *PLoS ONE*, vol. 9, no. 2, p. e87056, 2014.

[14] J. N. Mak *et al.*, "EEG correlates of P300-based brain-computer interface (BCI) performance in people with amyotrophic lateral sclerosis," *J. Neural Eng.*, vol. 9, no. 2, pp. 1–11, Apr. 2012.

[15] S. Makeig, "Blind separation of auditory event-related brain responses into independent components," *Proc. Nat. Acad. Sci. USA*, vol. 94, no. 20, pp. 10979–10984, 1997.

[16] K. J. Friston, "Functional connectivity: The principal-component analysis of large (PET) data sets," *J. Cerebral Blood Flow Metabolism*, vol. 13, no. 1, pp. 5–14, 1993.

[17] D. De Venuto and A. S. Vincentelli, "Dr. Frankenstein's dream made possible: Implanted electronic devices," in *Proc. Design, Autom. Test Eur. (DATE)*, Mar. 2013, pp. 1531–1536.

[18] D. De Venuto, D. T. Castro, Y. Ponomarev, and E. Stikvoort, "Low power 12-bit SAR ADC for autonomous wireless sensors network interface," in *Proc. 3rd Int. Workshop Adv. Sensors Int. (IWASI)*, 2009, pp. 1071–1075, doi: 10.1109/IWASI.2009.5184780.

[19] D. De Venuto, S. Carrara, and B. Riccò, "Design of an integrated low-noise read-out system for DNA capacitive sensors," *Microelectron. J.*, vol. 40, no. 9, pp. 1358–1365, 2009, doi: 10.1016/j.mejo.2008.07.071.

[20] D. De Venuto, V. F. Annese, M. Ruta, E. Di Sciascio, and A. L. S. Vincentelli, "Designing a cyber–physical system for fall prevention by cortico–muscular coupling detection," *IEEE Des. Test*, vol. 33, no. 3, pp. 66–76, Jun. 2016, doi: 10.1109/MDAT.2015.2480707.

[21] V. F. Annese, M. Crepaldi, D. Demarchi, and D. De Venuto, "A digital processor architecture for combined EEG/EMG falling risk prediction," in *Proc. Design, Autom. Test Eur. Conf. Exhibit. (DATE)*, 2016, pp. 714–719.

[22] V. F. Annese and D. De Venuto, "The truth machine of involuntary movement: FPGA based cortico-muscular analysis for fall prevention," in *Proc. IEEE Int. Symp. Signal Process. Inf. Technol. (ISSPIT)*, Dec. 2015, pp. 553–558, doi: 10.1109/ISSPIT.2015.7394398.

[23] M. de Tommaso, E. Vecchio, K. Ricci, A. Montemurno, D. De Venuto, and V. F. Annese, "Combined EEG/EMG evaluation during a novel dual task paradigm for gait analysis," in *Proc. 6th IEEE Int. Workshop Adv. Sensors Int. (IWASI)*, Jun. 2015, pp. 181–186, doi: 10.1109/IWASI.2015.7184949.

[24] C. C. Duncan *et al.*, "Event-related potentials in clinical research: Guidelines for eliciting, recording, and quantifying mismatch negativity, P300, and N400," *Clin. Neurophys.*, vol. 120, no. 11, pp. 1883–1908, 2009.

[25] V. Dinteren *et al.*, "P300 development across the lifespan: A systematic review and meta-analysis," *PLoS ONE*, vol. 9, no. 2, p. e87347, 2014.

[26] T. Frodl *et al.*, "Value of event-related P300 subcomponents in the clinical diagnosis of mild cognitive impairment and Alzheimer's disease," *Psychophysiology*, vol. 39, no. 2, pp. 175–181, 2002.

[27] C. D. Woody, "Characterization of an adaptive filter for the analysis of variable latency neuroelectric signals," *Med. Biol. Eng.*, vol. 5, no. 6, pp. 539–553, 1967.

[28] Y. Takeda, M.-A. Sato, K. Yamanaka, D. Nozaki, and Y. Yamamoto, "A generalized method to estimate waveforms common across trials from EEGs," *NeuroImage*, vol. 51, no. 2, pp. 629–641, 2010.

[29] G. Ouyang, W. Sommer, and C. Zhou, "A toolbox for residue iteration decomposition (RIDE)—A method for the decomposition, reconstruction, and single trial analysis of event related potentials," *J. Neurosci. Methods*, vol. 250, pp. 7–21, Jul. 2014.

[30] V. F. Annese and D. De Venuto, "Fall-risk assessment by combined movement related potentials and co-contraction index monitoring," in *Proc. IEEE Biomed. Circuits Syst. Conf., Eng. Healthy Minds Able Bodies (BioCAS)*, Oct. 2015, pp. 1–4, doi: 10.1109/BioCAS.2015.7348366.

[31] V. F. Annese and D. De Venuto, "Gait analysis for fall prediction using EMG triggered movement related potentials," in *Proc. 10th IEEE Int. Conf. Design Technol. Integr. Syst. Nanosc. Era (DTIS)*, Apr. 2015, pp. 1–6, doi: 10.1109/DTIS.2015.7127386.

[32] D. De Venuto and M. J. Ohletz, "On-chip test for mixed-signal ASICs using two-mode comparators with bias-programmable reference voltages," *J. Electron. Test., Theory Appl.*, vol. 17, nos. 3–4, pp. 243–253, 2001, doi: 10.1023/A:1013377811693.

[33] D. De Venuto, M. J. Ohletz, and B. Ricco, "Automatic repositioning technique for digital cell based window comparators and implementation within mixed-signal DfT schemes," in *Proc. Int. Symp. Quality Electron. Design (ISQED)*, Jan. 2003, pp. 431–437, doi: 10.1109/ISQED.2003.1194771.